Received: 30 May 2022 | Accepted: 17 August 2022

DOI: 10.1111/2041-210X.13981

Methods in Ecology and Evolution

RESEARCH ARTICLE

Active Remote Sensing for Ecology and Ecosystem Conservation

Tree species classification from complex laser scanning data in Mediterranean forests using deep learning

Matthew J. Allen[1] | Stuart W. D. Grieve[2,3] | Harry J. F. Owen[1] | Emily R. Lines[1]

[1]Department of Geography, University of Cambridge, Cambridge, UK

[2]School of Geography, Queen Mary University of London, London, UK

[3]Digital Environment Research Institute, Queen Mary University of London, London, UK

Correspondence
Matthew J. Allen
Email: mja78@cam.ac.uk

Funding information
UK Research and Innovation, Grant/Award Number: EP/S022961/1 and MR/T019832/1

Handling Editor: Carlos Alberto Silva

Abstract

1. Recent advances in terrestrial laser scanning (TLS) technology have enabled the automatic capture of three-dimensional vegetation structure at high resolution, but the scalability of using these data for large-scale forest monitoring is limited by reliance on intensive manual data processing, including the use of stem maps generated in the field to determine tree species. New methods from data science have the capacity to automate this identification process, reducing the hurdles towards automated inventories with TLS. In particular, contemporary developments in point cloud processing methods, alongside large increases in the computing power of consumer-level graphics processing units, provide new opportunities.
2. Here, we apply a deep learning-based approach, based on joint classification from multiple viewpoints for each stem, to automatically classify tree species directly from laser scanning data obtained in structurally complex Mediterranean forests. We also explore the use of data augmentation techniques to maximise performance for a fixed number of manually labelled stems. Our method does not require expensive pre-processing such as leaf-wood separation or quantitative reconstructions.
3. Using modern network architectures and data augmentation techniques, and without extensive pre-processing, we are able to achieve high overall and per-species accuracy that is comparable or higher than in existing work while using data from a water-limited ecosystem complicated by structural convergence and multi-stem trees.
4. Our findings demonstrate the power of deep learning to remove a major TLS data processing obstacle—individual species identification—and to minimise the bottleneck created by manual data labelling requirements in the use of TLS for standard forest monitoring.

KEYWORDS
convolutional neural networks, data augmentation, deep learning, forest monitoring, machine learning, terrestrial laser scanning, tree species classification, water-limited ecosystems

1 | INTRODUCTION

Reliable large-scale data on the state of forests are needed to monitor many aspects of forest structure and function, including ecosystem health (Pommerening & Grabarnik, 2019), carbon storage (Kurz et al., 2002) and the impacts of global change (Peñuelas et al., 2017). Such information can be obtained via plot data and national inventories (Burley et al., 2004), and typically comprises simple measurements such as diameter at breast height (DBH) and, perhaps, height, crown radius and depth (Burley et al., 2004). Allometric equations can then be used to estimate quantities of interest such as basal area and stand biomass (Kebede & Soromessa, 2018). These measurements and estimates may further be used, for example, to calculate merchantable timber (Kangas & Maltamo, 2006) or aboveground carbon storage (Talbot et al., 2014). Although these ground measurements are widely used, they come with many limitations; calculated quantities likely have substantial uncertainty due to the implicit approximations made by allometric equations (Wang, 2006), and they cannot capture fine-scale information such as variation in crown shape with depth, accurate cross-sectional shapes and branching structure. Detailed information on tree crown morphology is important for the study of forest dynamics such as competition between individual trees (Owen et al., 2021), and for accurate estimation of quantities such as branch biomass (Hu et al., 2021).

Recent advances in terrestrial laser scanning (TLS) mean that automatic capture of three-dimensional (3D) vegetation structure at high resolution is now possible (Wilkes et al., 2017). Because of its demonstrated high accuracy (Maas et al., 2008; Mengesha et al., 2014) and the additional metrics it can be used to calculate, there is substantial interest in the application of TLS to carry out inventories (Bienert et al., 2006; Liang et al., 2018; Piermattei et al., 2019; Simonse et al., 2003). However, while the use of TLS data to calculate simple metrics such as DBH, basal area and height, among others, is relatively straightforward once data are segmented into individual trees (Liang et al., 2016), major hurdles to large-scale implementation of TLS for surveying remain. One particular challenge is TLS data give only structural information, and the automated classification of stems into species or genus is not currently possible from raw point cloud data. This means that studies using TLS data must rely on stem maps generated in the field to identify species, to calculate any properties reliant on species information such as diversity, competitive interactions or specific wood density for carbon storage estimates. To address this, attempts have been made to classify tree species from TLS based on geometric features extracted after extensive data processing. For example, Terryn et al. (2020) used manually extracted structural features generated from quantitative structural models (QSMs; Raumonen et al., 2013) to classify five species of five different genera collected from a semi-natural western European woodland, obtaining a best overall classification accuracy of approximately 82%. However, while the use of manually specified features may increase interpretability of classification, this approach has drawbacks limiting both its scalability and wide applicability, since reducing information content to interpretable features in this may remove characteristics that improve classification, and the construction of QSMs is complex, relying on high point density raw data and manual refinement (Lau et al., 2018). In this study, we apply deep learning—the automated learning of the best features for downstream classification—to automate species identification from whole-tree TLS point clouds extracted from a dataset collected in Mediterranean woodland (Owen et al., 2021). Compared to a QSM-based approach, pre-processing requirements are substantially reduced and operator bias avoided, since feature choice is not pre-determined. We demonstrate that computer vision techniques (Hartley & Zisserman, 2003) and deep learning (LeCun et al., 2015) can be used to classify tree species from TLS point clouds from structurally mixed Mediterranean forests, with structurally complex features including multi-stems, potential structural convergence as a result of water limitation and significant variation in topographic conditions between individual plots.

TLS scanning generates point clouds—unordered sets of points in space representing a 3D shape or object—that are used in many areas of computer vision, including autonomous navigation (Zeng et al., 2018), robotics (Whitty et al., 2010) and forestry (Rahlf et al., 2021). Due to their wide range of applications, point clouds such as those generated by TLS systems have led to increasing attention in point cloud learning over the last decade, but applying machine learning to 3D data brings unique challenges compared to two-dimensional (2D) images (the standard domain of computer vision research); 3D point clouds are constructed by sampling irregularly in Cartesian space so are inherently non-Euclidean, meaning common deep learning techniques from 2D computer vision are not directly applicable. Although methods operating directly on point cloud data exist (Qi et al., 2017; Wang et al., 2019), they are often conceptually complex, difficult to implement and do not always outperform methods based on applying existing convolutional neural networks (CNNs) to projected images (Goyal et al., 2021; Seidel et al., 2021). We instead use a method based on joint classification of features extracted simultaneously from multiple 2D projections, henceforth referred to as 'SimpleView', which obviates the issue of building a network for point cloud data. This conceptually simple approach has been found to obtain state-of-the-art performance classifying exemplar laser scanning datasets (Goyal et al., 2021), and is likely agnostic to sensor resolution due to the abstraction of the input data from 3D point cloud to low-resolution 2D image.

Deep learning-based classification—the application of an unmodified architecture to a single orthographically projected image (mapping of a point cloud to a flat image)—has been applied for species classification from TLS data in plantation and unmanaged forests, with existing work focused on datasets with a small number species per genera. In managed plantations, Zou et al. (2017) classified species from TLS point cloud data by applying a single deep belief net (Hinton et al., 2006) to multiple projected views separately, achieving a maximum accuracy of 95.6% on data comprising eight species from eight distinct genera. Seidel et al. (2021) used a similar approach to classify TLS data from national parks and unmanaged forests in Germany and the United States into seven species of six

genera, with augmented samples appended to underrepresented classes before training. A simple network based on LeNet-5 (Lecun et al., 1998) achieved 86% overall accuracy, and compared positively to a pointwise approach, PointNet (Qi et al., 2017). Xi et al. (2020) benchmarked several models including voxel-based and point-based deep learning methods on a dataset of monospecific plots comprising nine species of five genera from Canada and Finland, with random augmentations applied during training, and achieved up to 95.8% overall accuracy with the best model. Existing work, however, is limited by its application to structurally simple data and by labour-intensive labelling requirements. Plantation forests such as those in Zou et al. (2017) lack the structural complexity of unmanaged forests, the use of monospecific plots by Xi et al. (2020) may have reduced structural variation in the data. Xi et al. (2020) achieve the best accuracy (95.8%), but used leaf-wood separated training data, which required between 1 and 10 h of manual labelling per tree, making this an impractical approach at scale.

Here we present a new approach, based on joint classification of multi-view 2D projections, to identifying species from segmented point cloud data, applied to a dataset of 2478 trees from unmanaged forests in central Spain containing five species of two genera (*Quercus* and *Pinus*, with species' sample sizes varying by up to an order of magnitude; Owen et al., 2021). The dataset used here is uniquely complex compared to previous studies, with multiple species in each genera represented, including species that hybridise (*Quercus ilex* and *Quercus faginea*), multi-stem individuals of all species, and collected in a plot network with both high seasonality and topographic variability likely causing structural convergence along both water and wind stress gradients (MacFarlane & Kane, 2017), potentially minimising structural differences between species. Furthermore, our approach requires minimal pre-processing and is not reliant on leaf-wood separated point clouds. We (1) assess whether our method can achieve high overall classification accuracy; (2) compare classification accuracies for individual species and assess whether higher classification accuracy is achieved between rather than within genera and (3) assess the extent to which data augmentation based on randomised transformations at train-time can improve performance and overcome unevenness in species sample sizes characteristic of forest data.

2 | MATERIALS AND METHODS

2.1 | Data

Our dataset comprises 2478 individual trees (Table 1) extracted from TLS scans taken in July 2018 in 38 30 × 30 m forest plots in central Spain—four in Cuellar (41.3°N, 4.2°W) and 34 in Alto Tajo Nature Reserve (40.9°N, 1.9°W). In Cuellar, plots were situated at 841 m above sea level in flat riparian zones, and were dominated by *Pinus pinaster* and *Pinus sylvestris*. Plots in Alto Tajo were between 960 m and 1400 m above sea level, and were dominated by four species—two oak (*Q. faginea*, *Q. ilex*) and two pine (*Pinus nigra*, *Pinus sylvestris*).

TABLE 1 Distribution of tree species from our dataset used to train/test the classifier. Individuals are classified as multi-stem if they bifurcated below 1.3 m (Owen et al., 2021)

Species	Total count	Multi-stem
Quercus faginea	1116	229
Pinus nigra	581	33
Quercus ilex	364	86
Pinus sylvestris	277	10
Pinus pinaster	140	1
Total	2478	359

See the main text and supplementary material of Owen et al. (2021) for further details. Plots were scanned using a Leica HDS6200 scanner, with scanner resolution set to 3.1 mm. In all, 16 scans spaced at 10 m in a grid pattern were used for each 30 × 30 m plot. Trees were automatically segmented from the data using the TREESEG package (Burt et al., 2018), followed by manual refinement on canopy trees; for full details of data collection and processing, see Owen et al. (2021). We discarded dead trees, species with low counts (less than 5 samples) and stems that were not identified or identified only to genus level, leaving five species—two *Pinus* and three *Quercus*. Exemplar individual tree scans of each of the five species used in this analysis are shown in Figure 1. Multi-stem trees are common in both *Quercus* species in this ecosystem (accounting for 21.3% overall), for example as a result of post-fire resprouting or past management, and a small number of *Pinus* trees of both species were also classified as multi-stem. Multi-stem trees were retained and not treated as separate classes within the analysis.

2.2 | Classification approach

2.2.1 | Camera projection and data pre-processing

Following Goyal et al. (2021), we used six camera projected images for each tree, since this approach, where projection lines are drawn from world point (the point in 3D coordinates projected onto the image) to camera point (the point at which the simulated camera is located in 3D coordinates), has been found to outperform orthographic projection, in which all projection lines are parallel to the image plane, when used for shape classification with this network architecture (Goyal et al., 2021). See Supplement 10 for projection details.

Individual tree point clouds were zero-centred by subtracting the mean and uniformly scaled to lie within $[-1, 1]^3$. The six camera projections were taken at a distance of 1.4 units. Axes are defined by the internal coordinate system of the scanner, where the *z*-axis is vertical and the *x*- and *y*- axes have no canonical direction (although they are consistent within each plot). Camera field of view (FOV) was set to 90° (as in Goyal et al., 2021) and image resolution was set to 256 × 256.

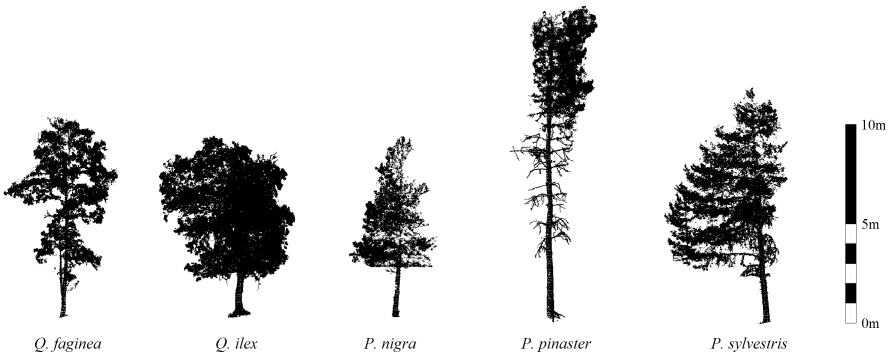

FIGURE 1 Example point clouds of each of the species in our dataset, before pre-processing; from left to right: *Quercus faginea*, *Quercus ilex*, *Pinus nigra*, *Pinus pinaster*, *Pinus sylvestris*.

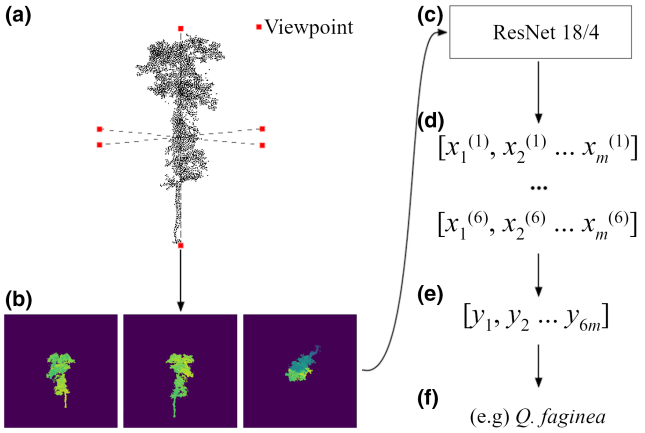

FIGURE 2 Overview of the projection and SimpleView network architecture. (a) Camera viewpoints for projection, shown with a *Quercus faginea* point cloud (downsampled); (b) example projections for a single tree. Six projections are made in total, with three not shown in this figure. Projection images are single channel and coloured yellow–green–blue for illustration only with yellow points being further away from the camera; (c) CNN (ResNet-18/4) taking six single channel projected images as input; (d) the CNN output vectors of extracted features (learned from the data); (e) feature vectors are concatenated into a single vector six times larger, and classification is performed based on this; (f) output layer is of length five, with each entry corresponding to the probability of the point cloud belonging to the corresponding species in our dataset. The species with the maximum probability is chosen as the prediction.

2.2.2 | Network architecture and protocol

We used the network architecture and training protocol SimpleView (Goyal et al., 2021), a simple method based on orthogonal camera projections that has been demonstrated to achieve near state-of-the-art performance on exemplar datasets of laser-scanned objects (Wu et al., 2015). Our architecture takes six images by camera projection along the axis directions—one from each of the positive and negative directions of the x, y, z axes (Figure 2a). We use the camera projection parameters from Goyal et al. (2021) throughout. Pixel values correspond linearly to depth, defined as the minimum distance to the camera along the camera axis where there is a point present in a pixel, and zero otherwise. This preserves some structural information in the direction parallel to the camera axis. Values are scaled such that the maximum depth for a given projection is 255, and a point with zero distance along the camera axis has a value of zero. These six images are then forward passed through a classification network (we use a ResNet18 with one-fourth filters, following Goyal et al., 2021) and the six sets of output features from this network—the values at the penultimate layer—are then fused via concatenation (found to give the better performance than pooling used in Goyal et al., 2021), and then classified. Intuitively—the network may learn to extract features such as height or crown depth from horizontal viewpoints, and crown diameter from vertical viewpoints. These features are considered simultaneously when classifying the species of the stem. In work such as Zou et al. (2017), a species is assigned directly to each individual viewpoint, and then a majority vote over all viewpoints is used to select the species. This has the disadvantage that ambiguous features from one perspective are treated with the same weight as features clearly corresponding to a single species from a different perspective of the same stem. A schematic of the method we used, SimpleView, is shown in Figure 2.

2.2.3 | Loss functions

Loss functions are used during the training of the network to assess current performance. Loss functions must be differentiable, and can be thought of as the 'distance' to the ground truth labels—with more accurate classifiers typically, but not always, having a lower loss. If a classifier frequently makes marginal, but incorrect, decisions between the correct label and another it is possible to obtain low loss simultaneously with low accuracy. In practice, this does not prevent the use of such functions to train networks. The value of the loss function is used as the minimisation target by the optimiser at each iteration during training. We used the smooth-loss (cross entropy with label smoothing) function from Goyal et al. (2021). For smooth-loss, where K is the number of classes, $\mathbf{t}$ is the vector truth label and $\mathbf{p}$ the vector of softmax probabilities:

$$\mathscr{L} = -\sum_{i=1}^{K} t_i \log(p_i). \quad (1)$$

Label smoothing is applied to a one-hot truth vector: $\mathbf{t}_{smooth} = (1-\varepsilon)\mathbf{t}_{1h} + \varepsilon / K$, where we use $\varepsilon = 0.2$ throughout. Goyal

et al. (2021) found smoothed labels outperform one-hot labels in all configurations on ModelNet classification, so we chose to use this loss function.

2.2.4 | Data augmentation

We perform data augmentation on-the-fly as stems are sampled from the dataset at train-time. This allows for a greater variety of augmented samples without increasing memory use, and may be particularly useful in ecological applications with many samples from common species and few from rare ones. When a stem is sampled from the dataset, the following random transformations are applied to the point cloud before projection: (1) random rotation around the vertical axis in the range $[0, R_{max}]$; (2) random translation in the range $[-T_{max}, T_{max}]^3$ and (3) random scaling in the range $[k_{min}, k_{max}]$. All augmentation hyperparameters (R_{max}, T_{max}, k_{min}, k_{max}) are optimised for best performance on the validation set. We performed classification with and without data augmentation, to compare if augmentation improved results compared to a baseline.

2.3 | Experimental configuration

A randomly selected train-validation-test split of 70%/15%/15% was used throughout. The same individual 70%/15%/15% of samples were used for training, validating and testing in all experiments, with the proportion of each species approximately even in all three sets. At train-time, weighted sampling with replacement was used to balance the dataset so that each species was equally represented. The Adam algorithm (Kingma & Ba, 2015) was used to optimise model parameters over 150 epochs. Learning rate was implemented using a step scheduler, of initial value l_0, decay γ and step size s, which were optimised jointly with data augmentation hyperparameters. We compare the accuracy (fraction of trees classified correctly) of the network trained with and without data augmentation applied, and use the same optimiser settings for both schemes. Typical train-times were of the order 30 min with pre-computed projections, and 5 h with on-the-fly projections (see system specifications below). Since we apply transformations whose parameters are sampled from a continuous space at train-time, rather than fixing these parameters in advance of training, the projections must also be computed at train-time; the majority of train-time was therefore spent performing projections rather than training the network.

Training hyperparameters (l_0, γ, s) were optimised jointly with augmentation hyperparameters (R_{max}, T_{max}, k_{min}, k_{max}) using Bayesian optimisation (Frazier, 2018) to maximise the highest model accuracy obtained on the validation dataset at any training epoch. For each model, we then report the best (at any epoch during training) model accuracy, as measured by performance on the test set (following Goyal et al., 2021). We also report the highest minimum producer accuracy obtained by any model during training. We calculate genus accuracies by aggregation—by predicting at the first species level, and scoring a prediction of any species in the same genus as the true label as correct. For example, a prediction of *Q. faginea* for a stem with true label *Q. ilex* is judged to be correct under this scheme.

All experiments are conducted on a local desktop computer running Ubuntu 20.04.1 LTS. The hardware used comprised an AMD Ryzen 93,900X 24-thread CPU, 64GB of system memory and a Nvidia RTX 2080Ti GPU with 11GB of video memory. Projections and network training were performed using PyTorch 1.8.1 (Paszke et al., 2019) and CUDA 11.1.

3 | RESULTS

3.1 | Hyperparameters

The optimised hyperparameters—parameters that govern the behaviour of the gradient descent algorithm and the maximum extent of transformations applied for data augmentation—obtained using Bayesian optimisation, are shown in Table 2. Hyperparameters were rounded to the nearest two decimal places or to the optimisation bounds if the final value was within 5%. Augmentation was found to produce the greatest increase in accuracy for rotation angles distributed around an entire turn rather than small angles, and a combination of scaling (scale factors $k_{min} = 0.71$, $k_{max} = 1.51$) and translation ($T_{max} = 0.93$) that keep most of the point cloud within the FOV of the camera. For context, a point at the same distance along the camera axis as the point (0,0,0) can be translated up to 1.4 units laterally before disappearing from view. The product of the maximum scale factor k_{max} and translation T_{max} is 1.404, so we expect approximately half of the point cloud to be cropped from the image in the most extreme case.

3.2 | Classification accuracy

We compared results from the same architecture with and without data augmentation, and found augmentation produced significant improvements. Corresponding overall, minimum producer and genus accuracies for the best overall and final models, and the model

TABLE 2 Optimised hyperparameters. Optimal hyperparameters for overall accuracy were the same as for the best producer accuracies

Optimiser	Augmentation					
Initial LR	Step size	Decay	Rotation	Translation	Scaling	
l_0	s	γ	R_{max}	T_{max}	k_{min}	k_{max}
0.001	86	0.82	2π	0.93	0.71	1.51

with the best minimum producer accuracy, are shown in Table 3. The highest overall accuracy obtained without augmentation was 69.3%, rising to 80.6% with data augmentation—an increase of 11.3%. With augmentation, we found an increase of 50% was observed in minimum producer accuracy—from 12.5% to 62.5%. We also calculated genus-level accuracies by aggregating the relevant entries of the confusion matrices in Figure 3—for example, for any true label in genus *Pinus*, a prediction of any *Pinus* species is considered to be correct, and likewise for *Quercus*—and found very high accuracy: 93.4% for *Pinus* and 91.2% for *Quercus* for the final model, which had the highest minimum producer accuracy at the genus level.

Confusion matrices for individual species prediction are shown in Figure 3 with and without data augmentation applied. Without augmentation, a large number of individuals were mistaken for *Q. faginea*—the most common species in our dataset. For the best overall model without augmentation, *Q. faginea* was the most frequent misclassification for two of the four remaining species, and three of the four remaining species for the final and best minimum producer

TABLE 3 Tabulated accuracy results for our classification approach. Within either the non-augmented or augmented schemes, all three models are from the same training run (so use the same hyperparameters). Model selection metric therefore refers to the metric used to select models (sets of optimised network weights) to be extracted from particular epochs during training. The best results for each metric under both the non-augmented and augmented schemes are shown in bold. We also calculated genus-level accuracies by aggregating the relevant entries of the confusion matrices in Figure 3—for example, for any true label in genus *Pinus*, a prediction of any *Pinus* species is considered to be correct, and likewise for *Quercus*. For example, to calculate the number of correct *Pinus* predictions from the confusion matrices, all entries in the top 3 × 3 sub-matrix are added, appropriately weighted by the number of samples in each species. The model achieving the best minimum species accuracy does not achieve the best minimum genus accuracy in our case

		Model selection metric (accuracy)	
		Best overall	**Best minimum producer**
Non-augmented data	Epoch	90	11
	Overall accuracy	**0.693**	0.663
	Minimum producer accuracy	0.042	**0.125**
	Pinus accuracy	0.753	0.633
	Quercus accuracy	0.945	0.958
Augmented data	Epoch	106	136
	Overall accuracy	**0.806**	0.751
	Minimum producer accuracy	0.300	**0.625**
	Pinus accuracy	0.883	0.961
	Quercus accuracy	0.975	0.864

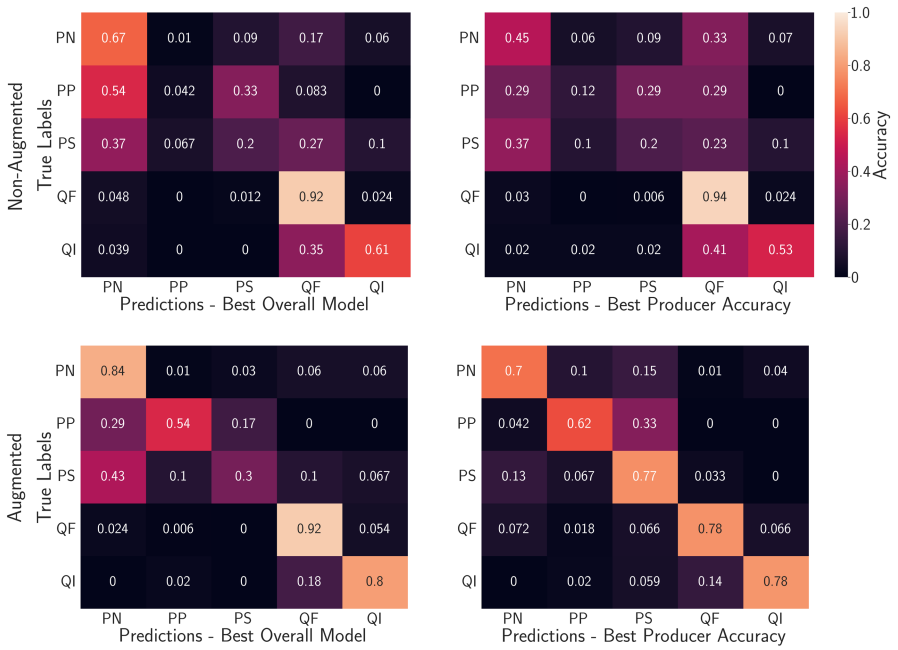

FIGURE 3 Confusion matrices for the best models as measured by the three metrics: (top row) without data augmentation and (bottom row) with data augmentation applied. The same colour bar applies in both cases. PN: *Pinus nigra*; PP: *Pinus pinaster*; PS: *Pinus sylvestris*; QF: *Quercus faginea*; QI: *Quercus ilex*.

accuracy models without augmentation. This confusion was not symmetric, as *Q. faginea* had 92% accuracy or more in all three models. This effect did not persist after the application of data augmentation, where species were more often mistaken for those within the same genus—for example, *P. pinaster* is mistaken for *P. nigra* and *P. sylvestris* in all three models, but is never mistaken for either *Quercus* species. For all species except *Q. faginea*, predictive accuracy was increased with data augmentation—by up to 57%, for *P. sylvestris* in the model with the best minimum species accuracy—across all three models. In the final model and the model with the best minimum species accuracy, the accuracy with which *Q. faginea* was classified decreased—by 17% and 16%, respectively—with augmentation.

4 | DISCUSSION

We found that our method, based on joint classification of multiple viewpoints, produced comparable accuracy to previous work in ecosystems uncomplicated by abiotic stressors and structural convergence when assessed per-species. When our classifications were aggregated to the genus level (see Section 3), we achieved accuracies of over 90% for both *Pinus* and *Quercus*, comparable to previous work in all ecosystems. A tabulated comparison of previous work classifying species from TLS data and our results are shown in Table 4. Our results were comparable to those requiring additional processing and subjective feature selection (Terryn et al., 2020), despite our use of data with multiple species-per-genus; classification based on learned features extracted automatically appears to yield better accuracies, as well as requiring substantially less manual input at the pre-processing stage. Requiring manual data processing presents substantial barriers to the uptake of TLS systems in standard forest monitoring; in addition to increasing labour requirements, tasks including the tuning of models such as QSMs require additional technical expertise. This necessitates the need for additional training or personnel as part of the forest monitoring process. Our approach presents fewer barriers to uptake of TLS systems in standard forest monitoring, and our results are comparable to those of others (e.g. Seidel et al., 2021)—despite the fact that our data are from an environment with significant abiotic variation that may create more intraspecific structural variation. Water limitation may affect tree structure by limiting height (Fajardo et al., 2019) and altering crown dimensions (Ding et al., 2020; Lines et al., 2012), leading to greater intraspecific variability across our plot network. The high topographic variability of our study area also means wind exposure varies between plots, inducing changes to tree structure (Watt et al., 2005), irrespective of drought conditions (Niez et al., 2019), potentially causing structural convergence between all species (MacFarlane & Kane, 2017). Individuals growing without abiotic stressors or exposed to homogeneous competitive conditions can grow into an architectural form that closely aligns with their phenotype and inherited developmental

TABLE 4 Tabulated comparison of our classifier versus existing work. 'Simultaneous multi-view perspective projections' refers to classification of multiple viewpoints based on extracting features from all projections without classifying each individual projection, then producing an overall classification based on considering features (e.g. the classifier may learn features such as height or crown width) from all projected images simultaneously. 'Sequential multi-view orthographic projections' refers to classifying each individual projection as a species, then taking a majority vote

Author	Ecosystem	Data	Method	Overall accuracy	Min. Species accuracy
This paper	Spanish (Mediterranean) woodland	5 Classes 5 Species 2 Genera 2478 Samples	Deep Learning (Simultaneous multi-view perspective projections)	0.81	0.62
Seidel et al. (2021)	German, US woodland	7 Classes 8 Species 6 Genera 690 Samples	Deep Learning (Single-view orthographic projection)	0.86	0.63
Terryn et al. (2020)	UK woodland (semi-natural)	5 Classes 5 Species 5 Genera 758 Samples	Support Vector Machines (Hand-crafted features)	0.82	0.58
Xi et al. (2020)	Canadian, Finnish woodland	9 Classes 9 Species 5 Genera 771 Samples	Deep Learning (Point-based, leaf-wood separated data)	0.96	0.71
Zou et al. (2017)	Chinese plantation forest	8 Classes 8 Species 8 Genera 40,000 Samples	Deep Learning (sequential multi-view orthographic projections)	0.96	0.95

programme (Horn, 1971; Pugnaire & Valladares, 2007), and studies in plantation forests (Zou et al., 2017) and with monospecific plots (Xi et al., 2020) are unlikely to exhibit the same structural convergence due to this lack of extrinsic stresses (MacFarlane & Kane, 2017; Martin-Ducup et al., 2020).

Data size, forest type and pre-processing efforts are likely to have driven the gap in performance between our work and that of Zou et al. (2017) and Xi et al. (2020). In the former case, substantially more data were used—an order of magnitude more than in our work, and two orders of magnitude more than in other work (Seidel et al., 2021; Terryn et al., 2020). Although obtaining and using large amounts of data is usually well advised when making use of deep learning, it is infeasible to gather such large datasets in many ecosystems. Furthermore, the data used in this case were gathered using mobile LiDAR mounted to a moving vehicle (Guan et al., 2015), which is not possible in most forests. The results presented by Xi et al. (2020) rely on leaf-wood segmented data, and the outlined approach relies on labelled training data which required 4–10 h of manual labelling per tree without assistance from a model, and 1–2 h per tree when model assisted (Xi et al., 2020). Supervised machine learning approaches to species classification from TLS data can only reduce the amount of required manual labour if producing the necessary volume of labelled training data takes less time than labelling the entire dataset by hand.

Data augmentation substantially reduced the impact of uneven species distribution in our data, improving accuracy of classification of less common species and maximising performance for the same number of manually labelled stems. Our findings suggest that this approach minimises the required data collection for a given level of performance and reduces bias introduced to predictions by unbalanced data. Using data augmentation, we were able to increase overall predictive accuracy (by 13%) without the need for additional data collection or processing. In the case of the model with the highest minimum producer accuracy, the minimum accuracy was increased from 12% to 62% (*P. pinaster*), with producer accuracies increasing for all but the most common species. The accuracy with which *Q. faginea* was correctly predicted decreased; it is overpredicted when data augmentation is not applied, owing to being overrepresented in the training set. This occurs despite the use of weighted sampling during training. After augmentation, confusion is more often between species of the same genus—we therefore suggest that the application of data augmentation reduces the effect of dataset bias on predictions, producing a model where predictive confusion is reflective of the functional similarity between species (which itself may reflect phylogenetic distance between species; Letten & Cornwell, 2015), so is inherent to the problem, rather than introduced artificially by unbalanced data. Minimising the required data labelling to achieve a given level of accuracy is an important step towards operationalising TLS in large-scale standard forest monitoring, and lower data labelling requirements mean our approach is also applicable at small to medium scales, unlike previous approaches relying on very large amounts of labelled data (Zou et al., 2017) or leaf-wood separated data (Xi et al., 2020). It may be possible to further reduce data requirements through use of transfer learning—either by training on existing data from other forest ecosystems and fine tuning on the target data or by use of more sophisticated techniques such as Model-Agnostic Meta Learning (Finn et al., 2017) if data from several ecosystems could be obtained collaboratively. Currently, labour-intensive labelled and segmented TLS data are not widely available. Making these data publicly available would be a significant step forward for the development of automated TLS processing methods, enabling the direct comparison of results across multiple ecosystems, in addition to transfer learning schemes. We make the data used in this work available for public use.

We found that the convergence of the classifier was somewhat unstable—large deviations in accuracy can be seen for each species across the two confusion matrices in Figure 3, despite the two models being selected from the same training run, using the same hyperparameters (seen in Table 1). This instability may be exaggerated by the size of the dataset—for example, given that there are 140 examples of *P. pinaster* in the data, it has approximately 20 samples in the validation set and a drop of 10% in species accuracy corresponds to misclassification of only two stems. Instability may also be caused by the hyperparameter selection process—particularly the joint optimisation of the model and optimiser hyperparameters. Maximum validation accuracy at any epoch was selected as the maximisation target, without regard to final accuracy; the gradient descent optimiser favours learning rates that offer rapid improvement within the allotted 150 epochs, but may overshoot optima to which it would converge at lower learning rates. We chose to allow this behaviour as a compromise to achieve the best performance within 150 epochs, with the number of epochs being limited by the large number of training runs needed to locate the best augmentation hyperparameters. In an operational setting, when only a single training run is required, running for a larger number of epochs would be appropriate to resolve this issue, as the scheduler decays the learning rate as training progresses. We were limited to a batch size of 128 trees (each with 6 images) by graphics processing unit memory constraints—increasing the batch size may improve the convergence of methods based on stochastic gradient descent (as gradient estimates based on small batches may be noisy), although this may come at the cost of decreased image resolution, which is likely to reduce classification accuracy (Koziarski & Cyganek, 2018; Sabottke & Spieler, 2020). Very large batches may also decrease the ability of the classifier to generalise from training to test data (Hoffer et al., 2017).

5 | CONCLUSIONS

Automatic species identification is one barrier to widespread uptake of TLS for forest monitoring, but others remain. For example, the full automation of the TLS data processing pipeline from plot to individual tree point clouds remains a major aim of the field. Although methods are available for semi-automatic segmentation of individual stems using generic point cloud processing techniques such as shape-fitting and clustering (Burt et al., 2018), a task focused approach using deep-learning may improve accuracy. A point-based

approach would be adaptable to segmentation in addition to classification. For example, Lv et al. (2021) achieved 86.6% classification accuracy on 1330 stems of four species from four genera by augmenting point cloud airborne laser scanning data with custom feature descriptors and applying a point-based network, PointNet++ (Qi et al., 2017), demonstrating that the use of point-based architectures is feasible with some modification. Xi et al. (2020) and Krisanski et al. (2021) make significant progress towards this goal, but are reliant on labour-intensive leaf-wood separated training data. To the best of our knowledge, there is no work performing instance segmentation on complex forest point clouds to jointly segment and classify individual trees by species in a single stage—although it is unclear whether this would offer benefits above a two-stage approach (separate segmentation and species classification), assuming both stages are automated.

The high classification accuracies achieved in this study demonstrate the strength of our approach—using deep learning architectures and data augmentation approaches from contemporary machine learning literature—and are an important step towards fully automated forest inventory, which would enable scalable long-term resource management and ecosystem conservation, improved inventory-based carbon storage estimates and greater understanding of ecological processes such as canopy and regeneration dynamics. Although untested here, our substantial downsampling of data from high-density TLS point clouds to 256×256 images suggests that lower quality TLS data may produce similar results. A method that is sensor agnostic and robust to varying data quality would be a major step forward to the scalability of TLS forest inventory, allowing faster data collection methods—such as backpack laser scanners—as well as simultaneously lowering the cost of data acquisition. We point to Krisanski et al. (2021) as an example of sensor agnostic methods for TLS data processing, although this work does not extend to species identification. The achieved high level of accuracy on structurally complex data is promising when considering whether this method will generalise to other ecosystems, although further investigation is required regarding performance in ecosystems with a very large number of species each with a smaller number of samples, such as in tropical forests. Large-scale data sharing initiatives would enable work on the automated processing of TLS data to be extended easily to multiple ecosystems. The cost of data acquisition could be further reduced if species identification methods could be adapted to not require stem maps as training labels—perhaps by transfer learning using openly available task-adjacent data such as RGB imagery (e.g. the iNaturalist dataset; Van Horn et al., 2017), rather than directly using projections from TLS data during training.

AUTHOR CONTRIBUTIONS

All authors conceived the idea; Matthew J. Allen and Emily R. Lines designed the methodology; Harry J. F. Owen collected and preprocessed the data; Matthew J. Allen analysed the data and led the writing of the manuscript. All authors contributed critically to the drafts and gave final approval for publication.

ACKNOWLEDGEMENTS

M.J.A. was supported by the UKRI Centre for Doctoral Training in Application of Artificial Intelligence to the study of Environmental Risks (EP/S022961/1). E.R.L., S.W.D.G. and H.J.F.O. were funded by a UKRI Future Leaders Fellowship awarded to E.R.L. (MR/T019832/1).

CONFLICT OF INTEREST

We declare that this research was conducted without any commercial or financial relationships that could be considered as conflicts of interest.

PEER REVIEW

The peer review history for this article is available at https://publons.com/publon/10.1111/2041-210X.13981.

DATA AVAILABILITY STATEMENT

Our data (Owen et al., 2021) are available for public use, and can be found at https://zenodo.org/record/6962717 (Owen et al., 2022). Code can be found at https://github.com/mataln/TLSpecies.

ORCID

Matthew J. Allen https://orcid.org/0000-0001-6877-6591
Stuart W. D. Grieve https://orcid.org/0000-0003-1893-7363
Harry J. F. Owen https://orcid.org/0000-0002-4294-1728
Emily R. Lines https://orcid.org/0000-0002-5357-8741

REFERENCES

Bienert, A., Scheller, S., Keane, E., Mullooly, G., & Mohank, F. (2006). Application of terrestrial laser scanners for the determination of forest inventory parameters. *International Archives of Photogrammetry, Remote Sensing and Spatial Information Sciences*, *36*(5).

Burley, J., Evans, J., & Youngquist, J. A. (2004). *Encyclopedia of forest sciences* (Vol. 1, p. 6502). Academic Press.

Burt, A., Disney, M., & Calders, K. (2018). Extracting individual trees from lidar point clouds using treeseg. *Methods in Ecology and Evolution*, *10*, 438–445. https://doi.org/10.1111/2041-210X.13121

Ding, J., Travers, S. K., & Eldridge, D. J. (2020). Grow wider canopies or thicker stems: Variable response of woody plants to increasing dryness. *Global Ecology and Biogeography*, *30*(1), 183–195. https://doi.org/10.1111/geb.13212

Fajardo, A., McIntire, E. J. B., & Olson, M. E. (2019). When short stature is an asset in trees. *Trends in Ecology & Evolution*, *34*(3), 193–199. https://doi.org/10.1016/j.tree.2018.10.011

Finn, C., Abbeel, P., & Levine, S. (2017). Model-agnostic meta-learning for fast adaptation of deep networks. *34th international conference on machine learning* (Vol. *70*). JMLR.org, 1126–1135. https://doi.org/10.48550/arXiv.1703.03400.

Frazier, P. I. (2018). *A tutorial on Bayesian optimization*. arXiv:1807.02811. arXiv. https://doi.org/10.48550/arXiv.1807.02811

Goyal, A., Law, H., Liu, B., Newell, A., & Deng, J. (2021). Revisiting point cloud shape classification with a simple and effective baseline. *International Conference on Machine Learning*, *139*, 3809–3820. https://doi.org/10.48550/arXiv.2106.05304

Guan, H., Yu, Y., Mi, W., Li, J., & Zhang, Q. (2015). Deep learning-based tree classification using mobile LiDAR data. *Remote Sensing Letters*, *6*, 864–873. https://doi.org/10.1080/2150704X.2015.1088668

Hartley, R., & Zisserman, A. (2003). *Multiple view geometry in computer vision* (p. 676). Cambridge University Press. https://doi.org/10.1017/CBO9780511811685

Hinton, G. E., Osindero, S., & Teh, Y.-W. (2006). A fast learning algorithm for deep belief nets. *Neural Computation*, *18*(7), 1527–1554. https://doi.org/10.1162/neco.2006.18.7.1527

Hoffer, E., Hubara, I., & Soudry, D. (2017). Train longer, generalize better: Closing the generalization gap in large batch training of neural networks. *Advances in Neural Information Processing Systems*, *30*, 1729–1739. https://doi.org/10.48550/arXiv.1705.08741

Horn, H. S. (1971). *The adaptive geometry of trees* (Vol. *3*). Princeton University Press. https://doi.org/10.2307/j.ctvx5w9x8

Hu, M., Pitkänen, T. P., Minunno, F., Tian, X., Lehtonen, A., & Mäkelä, A. (2021). A new method to estimate branch biomass from terrestrial laser scanning data by bridging tree structure models. *Annals of Botany*, *128*(6), 737–752. https://doi.org/10.1093/aob/mcab037

Kangas, A., & Maltamo, M. (2006). *Forest inventory: Methodology & applications* (Vol. *10*). Springer Dordrecht. https://doi.org/10.1007/1-4020-4381-3

Kebede, B., & Soromessa, T. (2018). Allometric equations for aboveground biomass estimation of *Olea europaea* L. subsp. cuspidata in Mana Angetu Forest. *Ecosystem Health and Sustainability*, *4*, 1–12. https://doi.org/10.1080/20964129.2018.1433951

Kingma, D. P., & Ba, J. (2015). Adam: A method for stochastic optimization. ICLR. arXiv. https://doi.org/10.48550/arXiv.1412.6980

Koziarski, M., & Cyganek, B. (2018). Impact of low resolution on image recognition with deep neural networks: An experimental study. *International Journal of Applied Mathematics and Computer Science*, *28*, 735–744. https://doi.org/10.2478/amcs-2018-0056

Krisanski, S., Taskhiri, M. S., Gonzalez Aracil, S., Herries, D., Muneri, A., Gurung, M. B., Montgomery, J., & Turner, P. (2021). Forest structural complexity tool—An open source, fully-automated tool for measuring forest point clouds. *Remote Sensing*, *13*(22), 4677. https://doi.org/10.3390/rs13224677

Kurz, W. A., Apps, M., Banfield, E., & Stinson, G. (2002). Forest carbon accounting at the operational scale. *The Forestry Chronicle*, *78*(5), 672–679. https://doi.org/10.5558/tfc78672-5

Lau, A., Bentley, L. P., Martius, C., Shenkin, A., Bartholomeus, H., Raumonen, P., Malhi, Y., Jackson, T., & Herold, M. (2018). Quantifying branch architecture of tropical trees using terrestrial LiDAR and 3D modelling. *Trees*, *32*(5), 1219–1231. https://doi.org/10.1007/s00468-018-1704-1

LeCun, Y., Bengio, Y., & Hinton, G. (2015). Deep learning. *Nature*, *521*(7553), 436–444. https://doi.org/10.1038/nature14539

Lecun, Y., Bottou, L., Bengio, Y., & Haffner, P. (1998). Gradient-based learning applied to document recognition. *Proceedings of the IEEE*, *86*(11), 2278–2324. https://doi.org/10.1109/5.726791

Letten, A. D., & Cornwell, W. K. (2015). Trees, branches and (square) roots: Why evolutionary relatedness is not linearly related to functional distance. *Methods in Ecology and Evolution*, *6*(4), 439–444. https://doi.org/10.1111/2041-210X.12237

Liang, X., Hyyppä, J., Kaartinen, H., Lehtomäki, M., Pyörälä, J., Pfeifer, N., Holopainen, M., Brolly, G., Francesco, P., Hackenberg, J., Huang, H., Jo, H.-W., Katoh, M., Liu, L., Mokroš, M., Morel, J., Olofsson, K., Poveda-Lopez, J., Trochta, J., … Wang, Y. (2018). International benchmarking of terrestrial laser scanning approaches for forest inventories. *ISPRS Journal of Photogrammetry and Remote Sensing*, *144*, 137–179. https://doi.org/10.1016/j.isprsjprs.2018.06.021

Liang, X., Kankare, V., Hyyppä, J., Wang, Y., Kukko, A., Haggrén, H., Yu, X., Kaartinen, H., Jaakkola, A., Guan, F., Holopainen, M., & Vastaranta, M. (2016). Terrestrial laser scanning in forest inventories. *ISPRS Journal of Photogrammetry and Remote Sensing*, *115*, 63–77. https://doi.org/10.1016/j.isprsjprs.2016.01.006

Lines, E. R., Zavala, M. A., Purves, D. W., & Coomes, D. A. (2012). Predictable changes in above ground allometry of trees along gradients of temperature, aridity and competition. *Global Ecology and Biogeography*, *21*(10), 1017–1028. https://doi.org/10.1111/j.1466-8238.2011.00746.x

Lv, Y., Zhang, Y., Dong, S., Yang, L., Zhang, Z., Li, Z., & Hu, S. (2021). A convex hull-based feature descriptor for learning tree species classification from als point clouds. *IEEE Geoscience and Remote Sensing Letters*, *19*, 1–5. https://doi.org/10.1109/LGRS.2021.3055773

Maas, H.-G., Bienert, A., Scheller, S., & Keane, E. (2008). Automatic forest inventory parameter determination from terrestrial laser scanner data. *International Journal of Remote Sensing*, *29*(5), 1579–1593. https://doi.org/10.1080/01431160701736406

MacFarlane, D. W., & Kane, B. (2017). Neighbour effects on tree architecture: Functional trade-offs balancing crown competitiveness with wind resistance. *Functional Ecology*, *31*(8), 1624–1636. https://doi.org/10.1111/1365-2435.12865

Martin-Ducup, O., Ploton, P., Barbier, N., Momo Takoudjou, S., Mofack, G., II, Kamdem, N. G., Fourcaud, T., Sonké, B., Couteron, P., & Pélissier, R. (2020). Terrestrial laser scanning reveals convergence of tree architecture with increasingly dominant crown canopy position. *Functional Ecology*, *34*(12), 2442–2452. https://doi.org/10.1111/1365-2435.13678

Mengesha, T., Hawkins, M., & Nieuwenhuis, M. (2014). Validation of terrestrial laser scanning data using conventional forest inventory methods. *European Journal of Forest Research*, *134*, 211–222. https://doi.org/10.1007/s10342-014-0844-0

Niez, B., Dlouha, J., Moulia, B., & Badel, E. (2019). Water-stressed or not, the mechanical acclimation is a priority requirement for trees. *Trees*, *33*(1), 279–291. https://doi.org/10.1007/s00468-018-1776-y

Owen, H. J. F., Flynn, W. R. M., & Lines, E. R. (2021). Competitive drivers of interspecific deviations of crown morphology from theoretical predictions measured with Terrestrial Laser Scanning. *Journal of Ecology*, *109*(7), 2612–2628. https://doi.org/10.1111/1365-2745.13670

Owen, H. J. F., Flynn, W. R. M., & Lines, E. R. (2022). Individual TLS tree clouds collected from both Alto Tajo and Cuellar in Spain. Version V1. *Zenodo*, https://doi.org/10.5281/zenodo.6962717

Paszke, A., Gross, S., Massa, F., Lerer, A., Bradbury, J., Chanan, G., Killeen, T., Lin, Z., Gimelshein, N., Antiga, L., Desmaison, A., Köpf, A., Yang, E., DeVito, Z., Raison, M., Tejani, A., Chilamkurthy, S., Steiner, B., Fang, L., … Chintala, S. (2019). Pytorch: An imperative style, high-performance deep learning library. *NeurIPS*, *32*, 8026–8037. https://doi.org/10.48550/arXiv.1912.01703

Peñuelas, J., Sardans, J., Filella, I., Estiarte, M., Llusià, J., Ogaya, R., Carnicer, J., Bartrons, M., Rivas-Ubach, A., Grau, O., Peguero, G., Margalef, O., Pla-Rabés, S., Stefanescu, C., Asensio, D., Preece, C., Liu, L., Verger, A., Barbeta, A., … Terradas, J. (2017). Impacts of global change on Mediterranean forests and their services. *Forests*, *8*(12), 463. https://doi.org/10.3390/f8120463

Piermattei, L., Karel, W., Wang, D., Wieser, M., Mokroš, M., Surový, P., Koren, M., Tomaštík, J., Pfeifer, N., & Hollaus, M. (2019). Terrestrial structure from motion photogrammetry for deriving forest inventory data. *Remote Sensing*, *11*(8), 950. https://doi.org/10.3390/rs11080950

Pommerening, A., & Grabarnik, P. (2019). *Individual-based methods in forest ecology and management* (1st ed.). Springer.

Pugnaire, F. I., & Valladares, F. (Eds.). (2007). *Functional plant ecology* (2nd ed., p. 744). CRC Press. https://doi.org/10.1201/9781420007626

Qi, C. R., Yi, L., Su, H., & Guibas, L. J. (2017). PointNet++: Deep hierarchical feature learning on point sets in a metric space. In *Proceedings of the 31st international conference on neural information processing systems* (pp. 5105–5114). Curran Associates Inc.

Rahlf, J., Hauglin, M., Astrup, R., & Breidenbach, J. (2021). Timber volume estimation based on airborne laser scanning — Comparing the use

of national forest inventory and forest management inventory data. *Annals of Forest Science*, *78*(2), 49. https://doi.org/10.1007/s13595-021-01061-4

Raumonen, P., Kaasalainen, M., Åkerblom, M., Kaasalainen, S., Kaartinen, H., Vastaranta, M., Holopainen, M., Disney, M., & Lewis, P. (2013). Fast automatic precision tree models from terrestrial laser scanner data. *Remote Sensing*, *5*(2), 491–520. https://doi.org/10.3390/rs5020491

Sabottke, C. F., & Spieler, B. M. (2020). The effect of image resolution on deep learning in radiography. *Radiology: Artificial Intelligence*, *2*(1), e190015. https://doi.org/10.1148/ryai.2019190015

Seidel, D., Annighöfer, P., Thielman, A., Seifert, Q. E., Thauer, J.-H., Glatthorn, J., Ehbrecht, M., Kneib, T., & Ammer, C. (2021). Predicting tree species from 3D laser scanning point clouds using deep learning. *Frontiers in Plant Science*, *12*, 635440. https://doi.org/10.3389/fpls.2021.635440

Simonse, M., Aschoff, T., Spiecker, H., & Thies, M. (2003). Automatic determination of forest inventory parameters using terrestrial laser-scanning. *ScandLaser Scientific Workshop on Airborne Laser Scanning of Forests*, *7*, 251–257.

Talbot, J., Lewis, S. L., Lopez-Gonzalez, G., Brienen, R. J. W., Monteagudo, A., Baker, T. R., Feldpausch, T. R., Malhi, Y., Vanderwel, M., Araujo Murakami, A., Arroyo, L. P., Chao, K.-J., Erwin, T., van der Heijden, G., Keeling, H., Killeen, T., Neill, D., Núñez Vargas, P., Parada Gutierrez, G. A., … Phillips, O. L. (2014). Methods to estimate aboveground wood productivity from long-term forest inventory plots. *Forest Ecology and Management*, *320*, 30–38. https://doi.org/10.1016/j.foreco.2014.02.021

Terryn, L., Calders, K., Disney, M., Origo, N., Malhi, Y., Newnham, G., Raumonen, P., Åkerblom, M., & Verbeeck, H. (2020). Tree species classification using structural features derived from terrestrial laser scanning. *ISPRS Journal of Photogrammetry and Remote Sensing*, *168*, 170–181. https://doi.org/10.1016/j.isprsjprs.2020.08.009

Van Horn, G., Mac Aodha, O., Song, Y., Cui, Y., Sun, C., Shepard, A., Adam, H., Perona, P., & Belongie, S. (2017). *The iNaturalist species classification and detection dataset*. https://doi.org/10.48550/ARXIV.1707.06642

Wang, C. (2006). Biomass allometric equations for 10 co-occurring tree species in Chinese temperate forests. *Forest Ecology and Management*, *222*(1), 9–16. https://doi.org/10.1016/j.foreco.2005.10.074

Wang, Y., Sun, Y., Liu, Z., Sarma, S. E., Bronstein, M. M., & Solomon, J. M. (2019). Dynamic graph CNN for learning on point clouds. *ACM Transactions on Graphics*, *38*(5), 146:1–146:12. https://doi.org/10.1145/3326362

Watt, M. S., Moore, J. R., & McKinlay, B. (2005). The influence of wind on branch characteristics of *Pinus radiata*. *Trees*, *19*(1), 58–65. https://doi.org/10.1007/s00468-004-0363-6

Whitty, M., Cossell, S., Dang, K., Guivant, J., & Katupitiya, J. (2010). Autonomous navigation using a real-time 3D point cloud. In *Australasian conference on robotics and automation*, pp. 1–3.

Wilkes, P., Lau, A., Disney, M., Calders, K., Burt, A., Gonzalez de Tanago, J., Bartholomeus, H., Brede, B., & Herold, M. (2017). Data acquisition considerations for Terrestrial Laser Scanning of forest plots. *Remote Sensing of Environment*, *196*, 140–153. https://doi.org/10.1016/j.rse.2017.04.030

Wu, Z., Song, S., Khosla, A., Yu, F., Zhang, L., Tang, X., & Xiao, J. (2015). 3D ShapeNets: A deep representation for volumetric shapes. In *IEEE Conference on computer vision and pattern recognition*, pp. 1912–1920. https://doi.org/10.1109/CVPR.2015.7298801

Xi, Z., Hopkinson, C., Rood, S. B., & Peddle, D. R. (2020). See the forest and the trees: Effective machine and deep learning algorithms for wood filtering and tree species classification from terrestrial laser scanning. *ISPRS Journal of Photogrammetry and Remote Sensing*, *168*, 1–16.

Zeng, Y., Hu, Y., Liu, S., Ye, J., Han, Y., Li, X., & Sun, N. (2018). RT3D: Real-time 3-D vehicle detection in lidar point cloud for autonomous driving. *IEEE Robotics and Automation Letters*, *3*(4), 3434–3440. https://doi.org/10.1109/LRA.2018.2852843

Zou, X., Cheng, M., Wang, C., Xia, Y., & Li, J. (2017). Tree classification in complex forest point clouds based on deep learning. *IEEE Geoscience and Remote Sensing Letters*, *14*(12), 2360–2364. https://doi.org/10.1109/LGRS.2017.2764938

SUPPORTING INFORMATION

Additional supporting information can be found online in the Supporting Information section at the end of this article.

How to cite this article: Allen, M. J., Grieve, S. W. D., Owen, H. J. F., & Lines, E. R. (2023). Tree species classification from complex laser scanning data in Mediterranean forests using deep learning. *Methods in Ecology and Evolution*, *14*, 1657–1667. https://doi.org/10.1111/2041-210X.13981